

# Extraction of Reliable Information from Time-Domain Pressure and Flow Signals Measured By Means of Forced Oscillation Techniques

RAOUL R. NIGMATULLIN<sup>1</sup>, SERGHEI I. OSOKIN<sup>1</sup>, CLARA IONESCU<sup>2</sup>, DUMITRU BALEANU<sup>3,4,5,\*</sup>

<sup>1</sup> Kazan (Volga region) Federal University, Institute of Physics, Kremlevskaya str.18, 420008, Kazan, Tatarstan, Russian Federation.

<sup>2</sup> Department of Electrical Energy, Systems and Automation, Ghent University, Technologiepark 913, 9052 Gent-Zwijnaarde, Belgium

<sup>3</sup> Department of Chemical and Materials Engineering, Faculty of Engineering, King Abdulaziz University, Jeddah, Saudi Arabia

<sup>4</sup> Department of Mathematics and Computer Science, Faculty of Art and Sciences, Cankaya University, 06530 Balgat, Ankara, Turkey

<sup>5</sup> Institute of Space Sciences, Magurele, 76911, Bucharest, Romania

*This paper aims to give a proof-of-concept for the possible application of the forced oscillation lung function test to assess the viscoelastic properties of the airways and tissue. In particular, a novel signal processing algorithm is employed on non-stationary, noisy, (relatively) short time series of respiratory pressure and flow signals. This novel technique is employed to filter the useful information from the signals acquired under two measurement conditions: pseudo-functional residual capacity (PFRC) and pseudo-total lung capacity (PTLC). The PFRC is the measurement performed at lowest lung volume with maximum deflation, and the PTLC is measurement performed at the maximum lung volume under maximum inflation. The results suggest that the proposed technique is able to extract information on the viscoelastic properties of the lung tissue at a macroscopic level. The conclusion of this preliminary study is that the proposed combination of signal processing method and lung function test is suited to be employed on a large database in order to deliver reference values and perform further statistical analysis.*

*Keywords: Respiratory mechanics, detrending procedure, filtering, lung function, oscillatory mechanics, statistical signal processing*

Within the context of healthy aging paradigm, ensuring an optimal lung function parameter follow-up is a key element in allowing early detection of respiratory disorders and managing treatment strategies to maximize their positive effect on the patient [1]. Periodical lung function testing provides a good insight into changes occurring in the airway resistance and tissue elasticity, allowing the clinicians to decide upon treatment updates for patient welfare. Lung function testing is aimed to be non-invasive, effective in assessing respiratory deficiencies and provide early detection of changes in the respiratory parameters to allow optimal treatment. Since most lung diseases affect the viscoelastic properties of the respiratory tissue [2,3], it is optimal that lung function tests provide information upon the intrinsic behaviour of lung tissue subjected to an external force.

Some of the most commonly used lung function test measurements are performed during forced inspirations and forced expirations, i.e. spirometry. A person's vital capacity can be measured by a spirometer [1,4]. The combination of several physiological measurements can help making a diagnosis of the underlying lung disease. Forced vital capacity (FVC) is the maximum volume of air that a person can exhale after maximum inhalation. Another important measure in spirometry is the forced expired volume in one second (FEV1). The FEV1/FVC ratio is used in the diagnosis of obstructive and restrictive lung disease, and normal values are approximately 80% [1,4]. In obstructive lung disease, the FEV1 is reduced due to obstruction to air escape. Thus, the FEV1/FVC ratio will be

reduced. However, these variations in (pressure and volume) are in fact a result of changing the viscoelastic properties of the respiratory airways and tissue.

The viscoelastic properties characterize materials such as polymers, found to be very similar to lung tissue [5]. In the human lung, these properties are changing with diseases and they may be detected at early stages by evaluating the respiratory impedance at low frequencies, i.e. closer to the breathing frequency of the patient [2,3,6]. However, the lower the frequency one wants to investigate in terms of signal processing methods, the more difficult the filtering problem between the breathing (which acts as a disturbance) and the effect of the excitation signal in the lungs (which is in fact the useful information one wants to extract). These complex problems could be avoided by performing tests in the absence of breathing, for short time series.

Recently, the interest in the lung function test by means of the forced oscillation technique (FOT) has been renewed and problems to be addressed have been identified and brought forward to the research community [7,8]. In particular, the problem of the non-stationary trend and nonlinear distortions present in the biological signals is of special interest [9].

The purpose of this paper is to present novel concepts of signal processing methods for analyzing time-domain pressure and flow measured during forced oscillations lung function test on three volunteers. Time-series analysis is a novel concept for the application of FOT, since typical results of FOT are frequency-domain respiratory

\* email: [dumitru@cankaya.edu.tr](mailto:dumitru@cankaya.edu.tr)

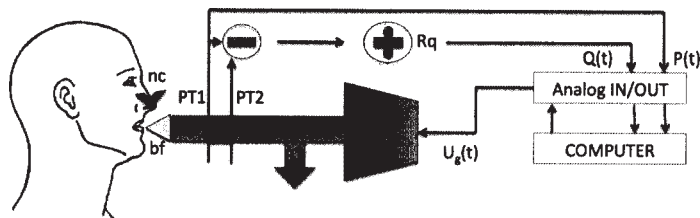


Fig. 1: (a) A photo and (b) a schematic overview of the FOT standard setup. Legend: LS - loudspeaker; BT - bias-tube; PN - pneumotachograph; PT1 and PT2 - pressure transducers; bf - biological filter with mouthpiece; nc - nose clip to prevent leakage of air-flow via the nose;  $R_q$  - known resistance in the pneumotachograph used to calculate flow;  $Q(t)$  - flow;  $P(t)$  - pressure;  $U_g(t)$  - multisine input generated using a loudspeaker (LS)

impedance values. Indeed, we also show that the measured signals are non-stationary and the proposed signal processing algorithm is able to deliver the underlying information.

Two measurement protocols are presented: i) when the lungs are inflated at their total capacity (PTLC), and ii) when they are deflated at their functional residual capacity (PFR). The extracted information is then provided by means of air-flow and air-volume in a limited time interval. The work presented in this paper provides a proof of the added value of FOT with respect to standard lung function testing and enables the use of FOT as a complementary lung function test to analyze the respiratory parameters.

The paper is organized as follows: the next section describes the measurement device and method, followed by the description of the signal processing algorithm. The third section presents the results for the two measurement protocols and a discussion section follows. The work is concluded in section 4 and some ideas for future applications are presented.

## Experimental part

### *FOT: applications, devices and respiratory signals measurement*

Medical devices for non-invasive lung function testing have been developed many decades ago. Some of them have been standardized and currently they are a part of the routine clinical tests. Among these, one can identify two classes of lung function tests: i) requiring patient cooperation for specific maneuvers, i.e. forced exhalation and forced inhalation; and ii) not requiring any special maneuvers from the patient, i.e. breathing at rest. The two standardized lung function tests from the first category are spirometry and body plethysmography [1], which are mainly extracting time domain respiratory signals as air-pressure, air-volume and air-flow and present the results as time-loops. The non-standardized lung function test from the second category is the forced oscillation technique [7,10], which also extracts time signals such as air-pressure and air-flow, but typically delivers the results in frequency domain representation, i.e. by means of the respiratory impedance [8,11].

Although standardized and currently used in clinical environment, spirometry has several limitations. It requires maximal, reproducible efforts, which in turn requires several measurement sessions from the patient, resulting in fatigue and time consumption. The maximal expiratory flow is dependent on the lung recoil pressure, the dynamic airway resistance and the airway properties at the flow saturation segment (i.e. flow plateau) [1,4]. Spirometry has also difficulties to clearly evaluate obstructive lung diseases. Even when paired with broncho-provocation, spirometry cannot reliably differentiate asthma and COPD

(chronic obstructive pulmonary disease) patients, and it is insensitive to early airway changes [12,13].

FOT is defined as superimposed external pressure signals on spontaneous breathing (tidal breathing) [11, 14, 15]. It provides an effort independent assessment of respiratory mechanics [7]. There is a significant amount of literature in pediatric applications (e.g. [15-19]) and there is an increasing interest in adult lung function testing [20]. Typically, the forced oscillations can employ a mono- or a multi-frequency excitation signal, typically in the range 4Hz to 30-50Hz. It can be continuous (eg. pseudo-random noise, optimized multisine), or time discrete (eg. impulse oscillations) [7, 10, 21, 22]. FOT has been broadly used for screening purposes, e.g. for detection of upper airway obstruction, small airways disease in COPD [23], during broncho-provocation tests [24], evaluation of vocal cord dysfunction [25], for assessment of bronchodilator response, and respiratory mechanics in obstructive sleep apnea [26].

The measurements of the signals analyzed in this paper have been performed using the device depicted in figure 1: the FOT standard setup, modified from a commercially available device. This is a commercially available I2M (Input Impedance Measurement) device previously produced by Chess Medical Technologies, Belgium, until 2005, nowadays the license is owned by COSMED, Italy. The specifications of the device are: 11 kg, 0.50x0.50x0.60 m, standard 8 seconds measurement time, European Directive 93/42 on Medical devices and safety standards EN60601-1. Because the standard measurement time (8 seconds) is too short to perform low frequency analysis, a second measurement line has been connected to a data acquisition card and the signals are recorded for 30 s, in order to provide better estimates. The subject is connected to the typical setup from figure 1 via a mouthpiece, suitably designed to avoid flow leakage at the mouth and dental resistance artifact.

In the device depicted in figure 1 the oscillatory pressure is generated by a loudspeaker (LS), which is connected to a chamber. The LS is driven by a power amplifier, controlled with the oscillating signal, which is in turn generated by a computer ( $U_g$ ). The movement of the LS cone generates a pressure oscillation inside the chamber, which is applied to the patient's respiratory system by means of a tube connecting the LS chamber and the bacterial filter (bf). A side opening of the main tubing (BT) allows the patient to have fresh air circulation. This pipeline has high impedance at the frequencies above 5 Hz to avoid the loss of power from the LS pressure chamber.

Before starting the measurements, the frequency responses of the transducers (PT) and of the pneumotachograph (PN) are calibrated. The measurements of air-pressure  $P$  and air-flow  $Q = dV/dt$

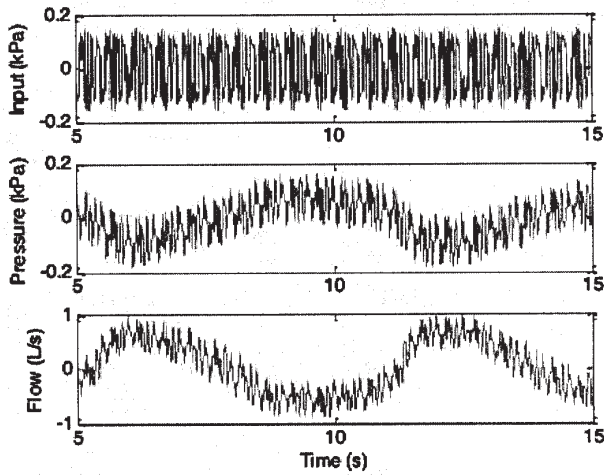


Fig. 2: Typical signals of pressure and flow measured during FOT test during normal breathing conditions.

(with  $V$  as the air volume) during the FOT lung function test is done at the mouth of the patient. The FOT excitation signal was kept within a range of a peak-to-peak size of 0.1-0.3 kPa in order to ensure optimality, patient comfort and linearity [8]. Measurements from three technically acceptable tests (i.e. no artifacts) were taken into consideration for each subject, with typical time-records depicted in figure 2. The measurements were reproducible and repeatability of the test protocol has been verified. The input is a multisine containing 5-50Hz excited frequency interval, pressure and flow are measured at the mouth of the patient, during normal breathing (i.e. observe the low frequency), showing the multisine super-imposed on the breathing signal. The time records were sampled at a sampling period of 500 Hz.

#### Volunteers and Measurement Protocol

In order to test our technique, three volunteers have been asked to perform the FOT test described in section 2.A and to follow the protocol described here below. To avoid the influence of non-homogeneity of the biometric data on the observations, the volunteers with similar bio-characteristics were chosen for measurements. Their biometric details are given in table 1. The lung function testing protocol followed in this study can be summarized as follows:

- a) the person breaths normally for 10 seconds, then it is asked to stop breathing with lungs deflated (PFR).
- b) the person repeats the same procedure as in a), but then with lungs inflated (PTLC).

#### Signal Processing Algorithm

For the treatment of the signals acquired by FOT, the POLS (procedure of the optimal linear smoothing) previously described in [27, 29] has been employed. When the initial measured data does not exhibit a visible trend, then it is useful to apply the POLS for the integrated curves. The latter are obtained from the initial curves by means of the trapezoid method with respect to their mean values. These curves are then calculated as in:

$$Dy_j = y_j - \langle y \rangle, \quad (1)$$

$$Jy_j = Jy_{j-1} + 0.5 \cdot (x_j - x_{j-1}) \cdot (Dy_{j-1} + Dy_j).$$

Volunteer	Age	Height	Weight
#1	32	175	76
#2	28	179	74
#3	31	165	67

where  $\langle \dots \rangle$  defines here and below the mean value,  $x_j$  is the normalized time  $x_j = t(j)/\max(t)$  and  $Jy_0 = 0$  defines the initial value of the integral with  $j=1, 2, \dots, N$ . The value of the optimal window  $w_{opt}$  is chosen from the conditions:

$$y_w = Gsm(x, y_w, w), \quad w' < w$$

$$RelErr(w) = \left[ \frac{\sigma(w)}{\text{mean}|y_w|} \right] \cdot 100\%$$

$$\sigma = Stdev(Dy) = \left[ \frac{1}{N} \sum_{j=1}^N (Dy_j)^2 \right]^{1/2} \quad (2)$$

$$\text{mean}(y) = \langle y \rangle = \frac{1}{N} \sum_{j=1}^N y_j$$

where the abbreviation  $Gsm(x, y, w)$  defines the linear smoothing operation,  $\langle \dots \rangle$  is the mean value and  $\sigma$  is the standard deviation of the signal.

$$Gsm(x_i, y_i, w) = \frac{\sum_{j=1}^N G\left(\frac{x_i - x_j}{w}\right) y_j}{\sum_{j=1}^N G\left(\frac{x_i - x_j}{w}\right)}, \quad G(x) = \exp\left(-\frac{x^2}{2}\right). \quad (3)$$

Notice that in (3) instead of initial random variable  $y_j$  we should use the preliminary smoothed variable  $Jy_j$  from (1). We want to stress here one principal point. Expression (2) should be considered as the iteration procedure realizing the successive smoothing in the limits of the given range of the smoothing window  $w \in [w_{min}, w_{max}]$ . Numerous tests show that the desired first local minima in behavior of the relative error (defined by expression (2)) is located in the interval  $[w_{min} = \text{Range}(x)/1000, w_{max} = \text{Range}(x)/10]$ , where  $\text{Range}(x) = \max(x) - \min(x)$ .

After calculation of the optimal trend for the integral curves one can use the same values of the optimal smoothing windows  $w$  calculated from expression (2) and then apply the POLS for initial data. In accordance with non-orthogonal amplitude-frequency analysis of the smoothed signals (NAFASS) [30] one can present the strongly-correlated smoothed sequence (signal  $S(t) = y(x)$  in our case) in the form of the finite combination of trigonometric functions:

$$S(t) \equiv F(t) = A_0 + \sum_{k=0}^{K-1} [Ac_k \cos(\omega_k t) + As_k \sin(\omega_k t)]. \quad (4)$$

where the frequency band  $w_k$  and the number of modes  $K$  ( $k=0, 1, \dots, K-1$ ) are found from the original procedure that is described in papers [30, 31]. The algorithm can be expressed in terms of a new set of variables  $Ac_k(w_k)$ ,  $As_k(w_k)$ , reducing the large number of the initially measured points  $N$  to the amplitude-frequency response with the total number of modes  $K \ll N$ . (Usually for the multi-periodic decomposition (4), the ratio  $N/K=30-40$ ).

$$NAFASS(S(t)) \equiv \{Ac_k(\omega_k), As_k(\omega_k)\} \quad (5)$$

Integration of relation (4) introduces terms that are proportional:  $\frac{\cos(\omega_k t)}{\omega_k}$  and  $\frac{\sin(\omega_k t)}{\omega_k}$ . These terms suppress

**Table 1**  
BIOMETRIC DETAILS FOR THE THREE VOLUNTEERS #3 WAS DIAGNOSED WITH CHRONIC BRONCHITIS AT THE TIME OF MEASUREMENT



the contribution of the high-frequency components for the integrated signal. Hence, the noise is eliminated from the signals and the integrated curves resulting from (1) can be used in an initial screening step for diagnostic purposes. The results of the methods employed in this treatment procedure are given in the next section.

The corresponding programs are original and were created in the frame of Mathcad14 software. The pseudo-code of the POLS approach is simple and can be divided in four steps.

**Step 1.** Set the initial and final limit values for the smoothing window:  $w_{\min} = \text{Range}(x)/1000$ ,  $w_{\max} = \text{Range}(x)/10$ ,  $\text{Range}(x) = \text{Max}(x) - \text{min}(x)$

$$w_i = w_{\min} + (i/K) (w_{\max} - w_{\min}), i=0,1,\dots,K$$

**Step 2.** Set the integrated value of random sequence from (1) as initial sequence  $nsm_0 = Jy_i$ .

**Step 3.** Realize the iteration procedure in accordance with expression (3)

$nsm_i = Gsm(x, nsm_{i-1}, w_i)$ , where  $nsm_i$  defines the calculated sequence at the given value of  $w_i$  from  $[w_{\min}, w_{\max}]$ .

**Step 4.** Calculate the value of the relative error  $\text{RelErr}(w_i)$  in accordance with (2) for all admissible values of  $w_i$  and find the first relative minima that provides its minimal value  $\text{min}(\text{RelErr}(w_{\text{opt}}))$ .

#### D. Statistical tests

In order to analyse whether or not there is a difference in measured signals between volunteers, and between

measurement protocols, statistical analysis was employed. ANOVA algorithm has been used for comparing the means of two or more columns of data, where each column represents an independent sample containing mutually independent observations (i.e. measurements of different volunteers).

#### Results and discussions

The results of the measurement protocol are given in figures 3-4 for Volunteer #1. The trend line in figure 3 shows that the pressure signal is stationary. The trend line in figure 4 shows that the flow signal is non-stationary. Similar results are obtained for volunteers #2 and #3.

The results of the measurements and the filtering techniques are summarized here. Figures 5-6 depict the flow and its integrated trend for the #1 and #2 volunteers during deflated lungs (PFRC). It can be observed that the trend is decreasing after some time, thereby suggesting the presence of creep and stress relaxation. Notice that results are similar qualitatively and quantitatively. Figure 7 depicts the same result, but for one volunteer with a chronic bronchitis, namely volunteer #3. It can be observed that both the shape and the values are changed. This implies that viscoelastic properties are changed and they can be detected with the POLS method.

The second part of the protocol implied that the procedure is repeated, but with inflated lungs in the absence of breathing. Figures 8-9 depict the results for the #1 and #2 volunteers without respiratory complaints, while figure 10 shows the result for the volunteer #3 with chronic bronchitis. In general, the values are higher for the

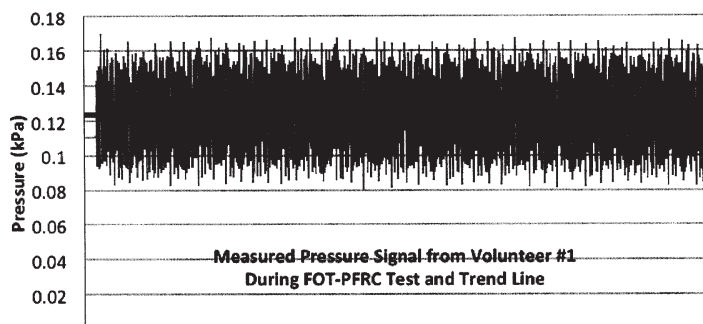


Fig. 3. Measured pressure signal during PFRC for volunteer #1.

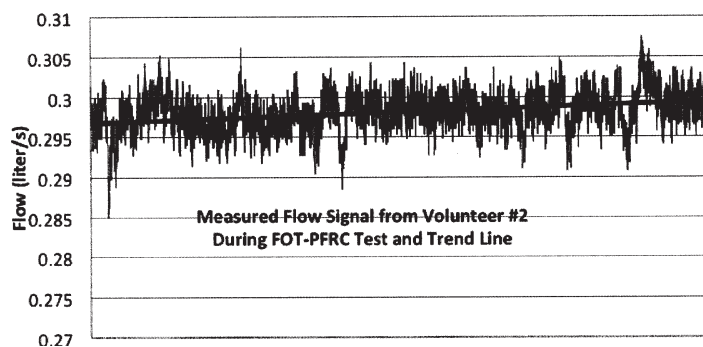


Fig. 4. Measured flow signal during PFRC for volunteer #2.

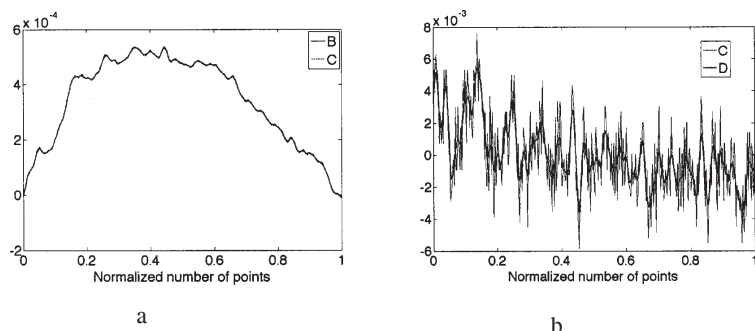


Fig. 5. (a) The integral of the flow (B) and its trend (C), respectively (b) the signal flow (C) and its trend (D), for volunteer #1 during PFRC. The trends are obtained by POLS method.

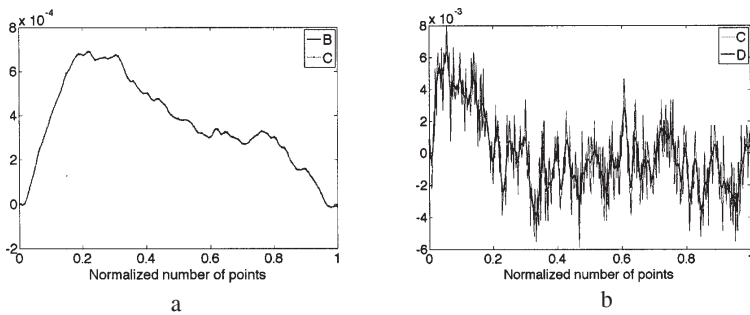


Fig. 6. (a) The integral of the flow (B) and its trend (C), respectively (b) the signal flow (C) and its trend (D), for volunteer #2 during PFRC. The trends are obtained by POLS method.

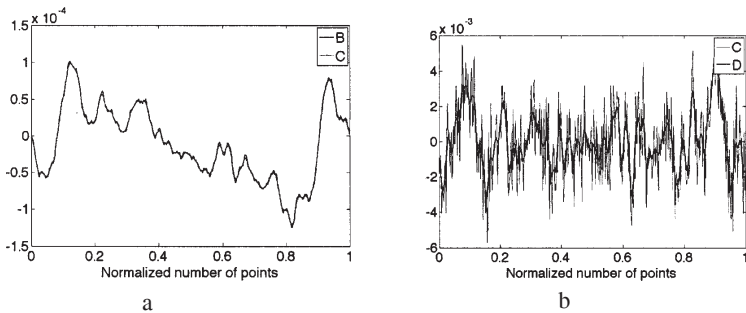


Fig. 7. (a) The integral of the flow (B) and its trend (C), respectively (b) the signal flow (C) and its trend (D), for volunteer #3 during PFRC. The trends are obtained by POLS method.

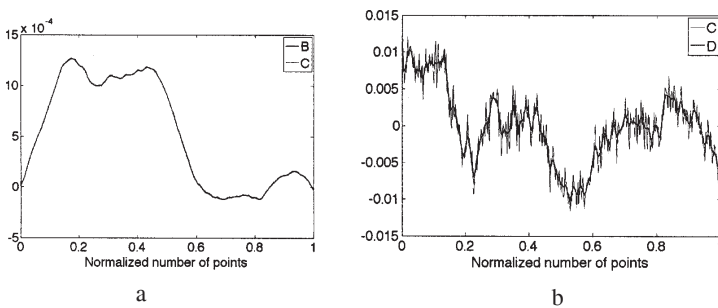


Fig. 8. (a) The integral of the flow (B) and its trend (C), respectively (b) the signal flow (C) and its trend (D), for volunteer #1 during PTLC. The trends are obtained by POLS method.

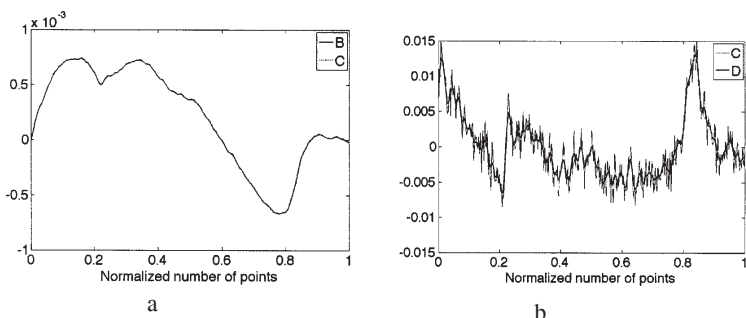


Fig. 9. (a) The integral of the flow (B) and its trend (C), respectively (b) the signal flow (C) and its trend (D), for volunteer #2 during PTLC. The trends are obtained by POLS method.

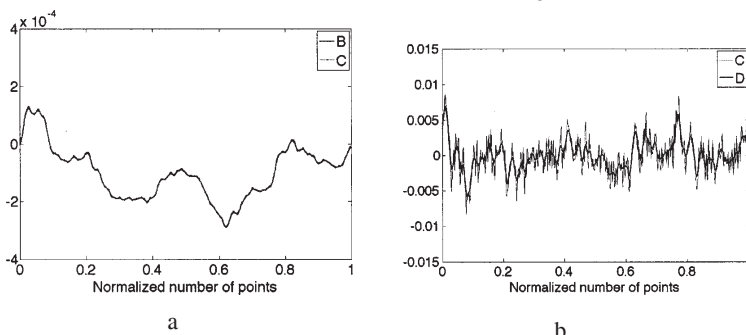


Fig. 10. (a) The integral of the flow (B) and its trend (C), respectively (b) the signal flow (C) and its trend (D), for volunteer #3 during PTLC. The trends are obtained by POLS method.

PTLC protocol since the lungs are now inflated. A similar observation as for PFRC can be made; i.e. the presence of viscoelastic effects and variation in the volunteer with respiratory complaint.

The ANOVA test has been employed to detect whether or not significant difference exists between the volunteers themselves. The result is given by means of a boxplot in figure 11, showing the trend extracted using POLS from the flow signal during FRC. The result suggests that the POLS method is able to detect differences in the volunteer #3, i.e. the one with chronic bronchitis ( $p < 0.05$ ).

FEV1 is a sensitive parameter diagnostic of lung disease, but its specificity is limited by the fact that a lower-than-expected value can indicate either that the airways are not as unobstructed as they should be (e.g. in asthma) or that there was a problem in expanding the lungs properly in the preceding maximal inspiration (e.g. restrictive pulmonary diseases as pulmonary fibrosis) [1,4]. This parameter is even more powerful when combined with a measure of the total volume of gas expired during an entire forced expiration, the FVC. Typically, both FVC and the ratio FEV1/FVC are lower than their normal values in obstructive diseases. In restrictive diseases, FVC is lower than normal,

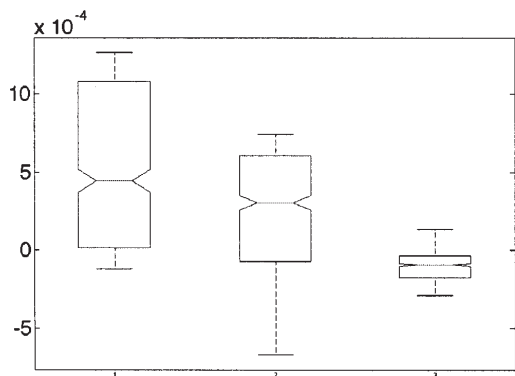


Fig. 11. Boxplot indicating that significant mean values are obtained between the volunteers #1 and #2 (left and middle columns), compared to volunteer #3 (right column).

but FEV1/FVC is usually preserved. The problem of these parameters is that they are not linked directly to lung structure and consequent changes with disease. This has motivated great efforts to develop macroscopic and microscopic models of lung viscoelasticity and mechanics.

All pulmonary diseases imply some kind of abnormality of lung tissue mechanics and thus changed viscoelastic properties. Complexity in lung mechanics arises because its behavior is not a simple reflection of the properties of its individual constituents (i.e. fibers, surfactant, cells). Main tissue mechanics originate from the manner in which these individual constituents are arranged, structured and interwoven with each other, resulting in complex interactions [2,3,33].

From a macroscopic perspective, the bulk elastic modulus of lung tissue is reflected in the relationship between inflation pressure and inhaled volume. This can be well compared to a rubber balloon. The tissue is also viscoelastic, because its elastic properties depend on the frequency to which volume is cycled (e.g. breathing patterns, multisine excitations) [2]. The dynamics of the bulk elastic recoil, evaluated at FRC, is dependent on the multiple interactions of fibers, cells and surfactant lipids and proteins within the geometry of the alveolus. During disease, the structure, geometry and thus interactions are not preserved. For instance, emphysema implies destruction of the alveolar tissue, leading a spongy aspect of the lung tissue reminiscent to a piece of Swiss cheese [3]. The size distribution of these holes can be well described by power laws, a feature arising ubiquitously in complex biological systems [3, 34]. Power law rheology in the lungs is best captured by fractional order differential equations [3,33] and fractional order lumped quasi-linear models [35]. These emerging tools from fractional calculus [36] have been successfully employed to distinguish between groups of healthy volunteers and asthma diagnosed patients [37], and between groups of healthy volunteers and patients diagnosed with chronic obstructive pulmonary disease [38]. Heterogeneity in the lung tissue has been also linked to the value of the fractional order in these lumped models [34].

When subject to a step constant stress, viscoelastic materials experience a time-dependent increase in strain. This phenomenon is known as viscoelastic creep. The stress relaxation is the decrease in strain value as a result of a constant stress. Typically, an oscillation applied at time  $t_0$  to the viscoelastic material will induce a response stress with a strain that increases. In the limit, for a continuous increase in stress, the material ultimately fails (i.e a resistance test). In the case of an oscillation, when the

stress is maintained for a shorter time period, the material undergoes an initial strain until a time  $t_1$  at which the stress is relieved, at which time the strain immediately decreases (discontinuity) then continues decreasing gradually to a residual strain. It has been shown in [39] that viscoelastic properties change the dynamics of breathing and time domain pressure and flow signals during FOT lung function tests.

Normal quiet breathing (such as during the forced oscillation technique lung function test) is accomplished by contraction of the diaphragm, the parasternal muscles and the scaleni. During inspiration, the diaphragm pulls the lower surfaces of the lung downwards. Expiration results from simple relaxation of these muscles. Changes in the elastic recoil of the lungs (more, or less, stiffness) will affect their normal function, in particular total lung volume and flow-volume relationships.

## Conclusions

The proposed combination of the signal processing method with the FOT lung function testing within the proposed protocol shows that information can be extracted about the amount of flow (and related pressure) at FRC and TLC conditions. If viscoelasticity of the lung tissue is to be analyzed, the method proposed herein can be employed to extract the trends of the signals from the measured signals. Figures 3-5 obtained in FRC conditions, show that the trend in the signal is behaving similarly to the creep and relaxation properties of viscoelastic materials. If this analysis would be employed on larger dataset (higher number of controls and diagnosed patients) the results may be used to detect variations in these viscoelastic properties from the measured respiratory signals.

*Acknowledgements: R.R. Nigmatullin and S.I. Osokin acknowledge the financial support within the framework of the research project "Dielectric spectroscopy and kinetics of complex systems" (Number: 12-18 02 0210 021000018) supported by Kazan Federal University (2012-2014). The authors want to express their sincere regards for a possibility to have interesting discussions with Dr. C.M. Ionescu from Flanders Research Centre, Belgium.*

## References

1. NORTHROP, R., Non-invasive measurements and devices for diagnosis, CRC Press, 2002.
2. BATES, J., Lung Mechanics - an inverse modelling approach, Cambridge University Press 2009.
3. SUKI, B., BATES, J., J. Appl. Physiol., **110**, 2011, p.1111.
4. PRIDE, N. B., Clin. Chest Med., **22**, 2001, p. 599.
5. LAKES, R., Viscoelastic Materials, Cambridge University Press, 2009.
6. LANDE, B., MITZNER, M., J. Appl. Physiol., **101**, 2006, p. 926.
7. BIRCH, M., MacLEOD, D., LEVINE, M., Phys. Meas., **22**, 2001, p.323.
8. OOSTVEEN, E., MacLEOD, D., LORINO, H., FARRÉ, R., ZANTOS, Z., DESAGER, K., MARCHAL, F., Eur. Respir. J., **22**, 2003, p.1026.
9. IONESCU, C.M., SCHOUKENS, J., De KEYSER, R., Detecting and analyzing non-linear effects in respiratory impedance measurements, American Control Conference, 29June-01 July, San Francisco, USA, ISBN 978-1-4577-0079-8, 2011, p. 5412.
10. SMITH, H. J., REINHOLD, P., GOLDMAN, M.D., Eur. Respir. Mon., **31**, 2005, p.72.
11. DUBOIS, A.B., BRODY, A.W., LEWIS, D. H., BURGESS Jr., B. F., J. Appl. Physiol., **8**, 1956, p.587.
12. FABBRI, L.M., ROMAGNOLI, M., CORBETTA, L., CASONI, G., BUSLJETIC, K., TURATO, G., LIGABUE, G., CIACCIA, A., SAETTA, M., PAPI, A., Am. J. Respir. Crit. Care Med., **167**, 2003, p. 418.
13. LAPPERRE, T., SNOECK-STROBAND, J. B., GOSMAN, M. M. E., STOLK, J., SONT, J. K., JANSEN, D.F., KERSTJENS, H.A.M., POSTMA, D.S., STERK, P.J., Am. J. Respir. Crit. Care Med., **170**, 2004, p.499.

14. RIGAU, J., FARRÉ, R., ROCA, J., MARCO, S., HERMS, A., NAVAJAS, D., *Eur. Respir. J.*, **19**, 2002, p.146.
15. SLY, P., HAYDEN, M., PETAK, F., HANTOS, Z., *Am. J. Respir. Crit. Care Med.*, **156**, 1996, p. 1172.
16. PETAK, F., BABIK, B., ASZTALOS, T., HALL, G., DEAK, Z., SLY, P., HANTOS, Z., *Pediatr. Pulmonology*, **35**, 2003, 169.
17. DELACOURT, C., LORINO, H., HERVE-GUILLOT, M., REINERT, P., HARF, A., Housset, B., *Am. J. Respir. Crit. Care Med.*, **161**, 2000, p.730.
18. BRENNAN, S., HALL, G., HORAK, F., MOELLER, A., PITREZ, P., FRANZAMANN, A., TURNER, S., de CLERCK, N., FRANKLIN, P., WINFIELD, K., BALDING, E., STICK, E., P. SLY P., *Thorax*, **60**, 2005, p.159.
19. DESAGER, K.N., BUHR, W., WILLEMEN, M., *J. Appl. Physiol.*, **71**, 1991., p.770.
20. Di MANGO, A.M., LOPES, A.J., JANSEN, J.M., MELO, P.L., *Respir. Med.*, **100**, 2006, p. 399.
21. JABLONSKI, I., MROCZKA, J., *Measurement*, **42**, 2009, p.390.
22. JABLONSKI, I., POLAK, A., MROCZKA, J., *Compt. Meth. Progr. Biomed.*, **101**, 2011, p.115.
23. HOGG, J.C., CHU, F., UTOKAPARCH, S., WOODS, R., ELLIOTT, M., BUZATU, L., CHERNIACK, R. M., ROGERS, R. M., SCIURBA, F. C., COXSON, H. O., PARÉ, P., *N. Engl. J. Med.*, **350**, 2004, p.2645.
24. EVANS, T.M., RUNDELL, K.W., BECK, K.C., LEVINE, A.M., BAUMANN, J.M., *J. Asthma*, **43**, 2006, p.49.
25. MORRIS, M. J., DEAL, L.E., BEAN, D.R., *Chest*, **116**, 1999, p.1676.
26. NAVAJAS, D., FARRÉ, R., ROTGER, M., BADIA, R., M., PUIG-DEMORALES, M. Montserrat, *Am. J. Respir. Crit. Care Med.*, **157**, 1998, p.1526.
27. NIGMATULLIN, R., *New Noninvasive Methods for Reading of Random Sequences and Their Applications in Nanotechnology*, chapter in book *New Trends in Nanotechnology and Fractional Calculus Applications*, Ed. D. Baleanu, Z. B. Guvenc, J.A. Tenreiro Machado, Springer, (2010) 43-56.
28. CIUREA, M. L., LAZANU, S., STAVARACHER, I., LEPADATU, A.M., V. IANCU, V., MITROI, M. R., NIGMATULLIN, R., BALEANU, C.M., *J. Applied Phys.*, **109**, 2011, 013717, DOI 10.1063/1.3525582
29. CETIN, S., BALEANU, C. M., NIGMATULLIN, R., BALEANU, D. OZCELIK, S., *Thin Solid Films*, **519**, 2011, p.5712.
30. NIGMATULLIN, R., OSOKIN, S., TOBOEV, V.A., *Chaos, Solit. Fract.*, **44**, 2011, p. 226.
31. NIGMATULLIN, R.R., *J. Appl. Nonl. Dyn.*, **1**, 2012, p.173.
32. NIGMATULLIN, R.R., BALEANU, D., AL-ZHRANI, A.A., ALHAMED, Y.A. ; ZAHID, A.H., YOUSSEF, T.E., *Rev.Chim (Bucuresti)*, **64**, no. 9, 2013, p.987
33. IONESCU, C. M., KOSINSKY, W., DE KEYSER, R., *Arch. Mechan.*, **62**, 2010, p. 21.
34. FREDBERG, J., STAMENOVIC, D., *J. Appl. Physiol.*, **67**, 1989, p.2408.
35. IONESCU, C. M., De KEYSER, R., DESAGER, K.N., DEROM, E., *Fractional-Order Models for Characterizing the Impedance of the Respiratory System*, G. Naik (Ed.), chapter 9 in book: *Advances in Biomedical Engineering 377-396*, ISBN 978-953-307-004-9, [www.intechweb.org/books.php](http://www.intechweb.org/books.php) (open access) ,2009.
36. WEST, B.J., *Fractal physiology and chaos in medicine, Studies of nonlinear phenomena in life sciences, vol.1.* Singapore: World Scientific ,1990.
37. IONESCU, C. M., DESAGER, K.N., De KEYSER, R., *Comput. Meth. Progr. Biomed.*, **101**, 2011, p. 315.
38. IONESCU, C.M., DEROM, E., DE KEYSER, R., *Comput. Meth. Progr. Biomed.* **97**, 2010, p.78.
39. IONESCU, C.M., *The human respiratory system: an analysis of the interplay between anatomy, structure, breathing and fractal dynamics*, Springer, Series in BioEngineering 2013, Print ISBN 978-1-4471-5387-0, Online ISBN 978-1-4471-5388-7.

---

Manuscript received: 19.12.2013